

## The Stability of $L_3$ Sponge Phase in Acidic Solutions

Shilpa H. Bhansali, Abds-Sami Malik, Jessica M. Jarvis, Ilke Akartuna, Daniel M. Dabbs, Jeffrey D. Carbeck, and Ilhan A. Aksay\*

Department of Chemical Engineering, Princeton University, Princeton, New Jersey 08544-5263

Received August 17, 2005

In the synthesis of the disordered lyotropic liquid crystalline  $L_3$  sponge phase prepared with the cosurfactants cetylpyridinium chloride and hexanol, aqueous NaCl solution is used as the solvent. When this sponge phase is used as the template for  $L_3$  silica-phase processing, we replace NaCl with HCl to facilitate the acid catalysis of tetramethoxysilane in forming a templated silica gel, assuming that changing the solvent from NaCl(aq) to HCl(aq) of equivalent ionic strength does not affect the stability range of the  $L_3$  phase. In this work, we confirm that changing the pH of the solvent from neutral to acidic (with HCl) has negligible effect on the  $L_3$  phase region. Equivalent ionic strength is provided by either NaCl(aq) or HCl(aq) solvent; therefore, a similar phase behavior is observed regardless of which aqueous solvent is used.

### Introduction

Amphiphilic surfactant molecules assemble into various spatially organized structures including one-dimensional spherical micelles, two-dimensional sheetlike smectic mesophases, and three-dimensional cubic and hexagonal matrixes.<sup>1,2</sup> The stability of the phases depends on the surfactant concentration, solution composition, solution ionic strength, and temperature.<sup>1–5</sup> Surfactant mesophases have been used as templates for synthesizing mesostructured organic–inorganic composites.<sup>6–8</sup> These templated materials have found applications in biological separations,<sup>9</sup> as catalysts and catalyst supports,<sup>10</sup> and as membranes.<sup>9</sup> A particularly interesting structure is the  $L_3$  or “sponge” phase that exists in the quasi-ternary system composed of cetylpyridinium chloride, hexanol, and 0.2 M (aq) NaCl or HCl solvent (Figure 1).<sup>11</sup> The  $L_3$  phase is a disordered isotropic structure that fills the volume of the liquid-crystalline solution (Figure 2).<sup>1</sup> The distorted bilayer forms two interpenetrating networks of channels ideal for the transport of materials throughout the structure. Characteristic to the liquid-crystalline  $L_3$  phase is the universal scaling law.<sup>1,11</sup> For a system that follows the universal scaling law, the topological form of the system remains unchanged when diluted with solvent and the characteristic distance increases linearly as a function of the reciprocal of the membrane volume fraction.<sup>11</sup> Such systems are known to be self-similar as they appear identical at all length scales.

We have previously used the  $L_3$  phase of the cetylpyridinium chloride monohydrate ( $\text{CpCl}\cdot\text{H}_2\text{O}$ ) surfactant/hexanol cosurfactant/0.2 M HCl(aq) system to synthesize templated silica

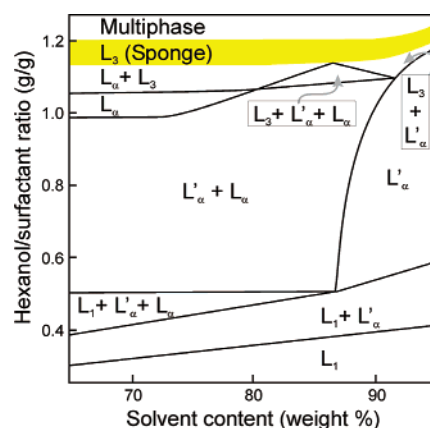


**Figure 1.** Phase diagram as determined by McGrath (ref 11) for the  $\text{CpCl}\cdot\text{H}_2\text{O}$ , NaCl(aq), and hexanol system. The quasi-ternary has been reduced to a pseudo-binary phase diagram by using the ratio of the co-surfactants to define the vertical axis. The  $L_3$  phase region is highlighted in yellow.

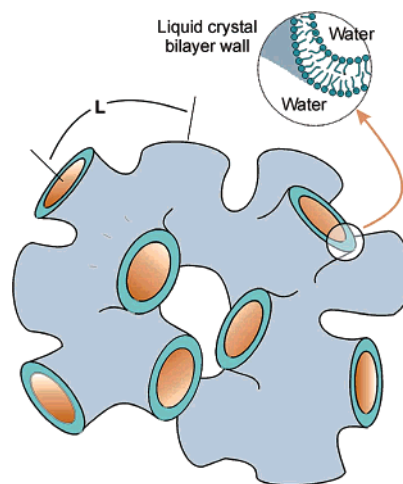


**Figure 2.** Schematic of  $L_3$  crystalline phase (modified from ref 1).

gels.<sup>12,13</sup> For this purpose, we replaced the brine solution (0.2 M NaCl) used by McGrath<sup>11</sup> with a 0.2 M HCl solvent in order

\* To whom correspondence should be addressed. E-mail: iaksay@princeton.edu.

- (1) Porte, G. *J. Phys. Condens. Matter* **1992**, *4*, 8649–8670.
- (2) Roux, D.; Coulon, C. *J. Phys. Chem.* **1992**, *96*, 4174–4187.
- (3) Anderson, D.; Wennerstrom, H.; Olsson, U. *J. Phys. Chem.* **1989**, *93*, 4243–4253.
- (4) Gomati, R.; Daoud, M.; Gharbi, A. *Physica B* **1997**, *239*, 405–412.
- (5) Gomati, R.; Appell, J.; Bassereau, P.; Marignan, J.; Porte, G. *J. Phys. Chem.* **1987**, *91*, 6203–6210.
- (6) Beck, J. S.; Vartuli, J. C.; Roth, W. J.; Leonowicz, M. E.; Kresge, C. T.; Schmitt, C.; Chu, T.-W.; Olson, K. H.; Sheppard, E. W.; McCullen, S. B.; Higgins, J. B.; Schlenker, J. L. *J. Am. Chem. Soc.* **1992**, *114*, 10834–10843.
- (7) Kresge, C. T.; Leonowicz, M. E.; Roth, W. J.; Vartuli, J. C.; Beck, J. S. *Nature* **1992**, *359*, 710–712.
- (8) Kim, S. S.; Zhang, W.; Pinnavaia, T. J. *Science* **1998**, *282*, 1302–1305.
- (9) Davis, M. E. *Nature* **1993**, *364*, 391–393.
- (10) Maschmeyer, T. *Curr. Opin. Solid State Mater. Sci.* **1998**, *3*, 71–78.
- (11) McGrath, K. M. *Langmuir* **1997**, *13*, 1987–1995.

- (12) McGrath, K. M.; Dabbs, D. M.; Yao, N.; Aksay, I. A.; Gruner, S. M. *Science* **1997**, *277*, 552–556.

to facilitate the hydrolysis of the silica precursor. The stability of the surfactant mesophase is critical in retaining the desired structure during templation, ensuring that the structure of the surfactant phase is reproduced in the inorganic phase.<sup>8</sup> While synthesizing  $L_3$ -templated silica, we noted that it was difficult to consistently synthesize silica gels in the concentrated regime of the phase diagram (55 wt% < solvent fraction < 65 wt%).

We attributed these inconsistencies in the synthesis of the  $L_3$ -templated silica to be due to (1) the  $L_3$  template used in the preparation of these gels was not prepared in the  $L_3$  phase domain and/or (2) addition of TMOS to synthesize the silica gel was possibly pushing the system out of the  $L_3$  phase field. Our experimental observations supported the former since we noted that some solutions appeared turbid and showed optical birefringence under cross-polarizer optics, contrary to the low viscosity, optically clear solution expected of an  $L_3$  phase, despite using a hexanol/CpCl $\cdot$ H $_2$ O ratio (h/c) of 1.15 consistent with the previously published phase diagram.<sup>11,14</sup> Further, samples that were characterized to have the  $L_3$  structure went on to generate  $L_3$ -templated silica gels, as determined by small-angle X-ray scattering (SAXS).<sup>15,16</sup>

When replacing a 0.2 M NaCl solvent with a 0.2 M HCl solvent, we alter the pH of the lyotropic liquid crystal. The Helfrich model for bilayer phases indicates that altering the electrostatics of a surfactant system by changing the pH of the solvent can result in a phase transformation.<sup>17,18</sup> The bending energy of a bilayer is dependent on the mean curvature modulus,  $K$ , and the Gaussian curvature modulus,  $\bar{K}$ .<sup>18</sup> Strongly negative values of  $\bar{K}$  favor the formation of disconnected micellar structures, whereas positive values favor the formation of a multiconnected, large aggregate structure.<sup>1</sup> The charge density on a surfactant membrane surface can affect both the bending rigidity ( $K_M$ ) as well as the Gaussian curvature of the bilayer ( $\bar{K}_M$ ).<sup>17</sup> In the Poisson–Boltzmann regime, the electrical contribution can lower the Debye length, resulting in a greater effect on  $\bar{K}_M$  than on  $K_M$ .  $\bar{K}_M$  becomes negative as a result of the excess ions on the outside of the bilayer and thus can be the cause of a phase transformation.

Effect of pH on the curvature of surfactants, as well as lipid membranes, has been experimentally observed and explained by the effects of surface charge on the membrane.<sup>19,20</sup> Hauser et al. showed the formation of unilamellar vesicles from a lamellar lipid film with an increase in the pH.<sup>19,20</sup> They implied that the spontaneous vesiculation is a result of the ionization of the phosphate group of the phospholipids on the outer monolayer of the bilayer. The phosphate group on the inner monolayer remains partially ionized, resulting in the formation of small vesicles from the large bilayer sheets.<sup>20</sup> Pinazo et al. recently showed a vesicle-to-ribbon transition behavior in diacyl glycerol amino acid-based surfactants.<sup>21</sup> They show that reducing the pH of the medium has the same effect as increasing the concentration of the surfactant: both result in a transformation from a vesicle form to a ribbonlike structure. The phase transition as a result of the decrease in pH alters the protonation of the surfactant,

(13) McGrath, K. M.; Dabbs, D. M.; Yao, N.; Edler, K. J.; Aksay, I. A.; Gruner, S. M. *Langmuir* **2000**, *16*, 398–406.

(14) Gomati, R.; Bouguerra, N.; Gharbi, A. *Physica B* **2002**, *322*, 262–269.

(15) Bhansali, S. H.; Jarvis, J. M.; Aksay, I. A.; Carbeck, J. D. Enhanced Resonator Sensitivity with Nanostructured Porous Silica Coatings. *Langmuir* **2006**, submitted for publication.

(16) Bhansali, S. H.; Woll, A.; Gruner, S. M.; Carbeck, J. D.; Aksay, I. A. Process Induced Variations in the Structure of  $L_3$ -Templated Silica Films, manuscript in preparation.

(17) Helfrich, W. *Phys. Lett. A* **1973**, *43*, 409–410.

(18) Helfrich, W. *J. Phys. Condens. Matter* **1994**, *6*, A79–A92.

(19) Hauser, H.; Gains, N. *Proc. Natl. Acad. Sci. U.S.A.* **1982**, *79*, 1683–1687.

(20) Hauser, H. *Proc. Natl. Acad. Sci. U.S.A.* **1989**, *86*, 5351–5355.

(21) Pinazo, A.; Perez, L.; Infante, M. R.; Pous, R. *Phys. Chem. Chem. Phys.* **2004**, *6*, 1475–1481.

**Table 1. Reagent Quantities used for Some Specific Samples<sup>a</sup>**

sample no.	solvent wt%	hexanol (g)	CpCl $\cdot$ H $_2$ O (g)	0.2 M HCl (g)	0.2 M NaCl (g)
1	95	0.136	0.115	4.756	
2	85	0.343	0.305	3.677	
3	75	0.669	0.576	3.738	
4	65	0.932	0.824	3.262	
5	95	0.133	0.106		4.564
6	85	0.368	0.310		3.853
7	75	0.630	0.565		3.608
8	65	0.930	0.797		3.213

<sup>a</sup> All reagents were measured gravimetrically. The weight percent solvent refers to the amount of 0.2 M HCl or 0.2 M NaCl used and was calculated by taking the quotient of the weight of 0.2 M HCl or NaCl over the sum of all reagent weights.

thereby increasing the surfactant-headgroup area and changing the bilayer curvature.<sup>21</sup> In view of these studies, we have deemed it essential to map the  $L_3$  phase domain for the (CpCl $\cdot$ H $_2$ O)/hexanol/0.2 M HCl(aq) and (CpCl $\cdot$ H $_2$ O)/hexanol/0.2 M NaCl(aq) to determine the role of pH on the  $L_3$  phase domain.

### Experimental Details

All solutions were prepared in air at room temperature. Cetylpyridinium chloride monohydrate [(C $_{16}$ H $_{33}$ C $_5$ H $_5$ N) $^+$ Cl $^-$  $\cdot$ H $_2$ O], hexanol, NaCl, (99%; Aldrich Chemical Co. Inc., Sheboygan Falls, WI) and HCl (1 part standard 1.0 N solution, Acros Organics, Morris Plains, NJ, to 4 parts deionized water) were stored at room temperature in air and used as received.

All reagent quantities were measured gravimetrically into the reaction vessel in order to ensure accuracy and reproducibility of the results. The liquid-crystal solutions were made in 20-mL vials with screw-top caps, first mixing hexanol with surfactant, using a Teflon coated stir bar, and making a paste such that the CpCl $\cdot$ H $_2$ O was completely wetted by the hexanol. Subsequently, the HCl(aq) solvent was added, the vial capped, and the solution mixed for  $\sim$ 20 min using a Teflon-coated stir bar. An identical procedure was followed to form the liquid crystal with 0.2 M NaCl(aq) as the solvent.

The reagent quantities used for representative samples are given in Table 1. For example, a solution containing 95 wt% solvent was made by first putting 0.115 g of CpCl $\cdot$ H $_2$ O in a reaction vial, to which 0.136 g hexanol was added. After being mixed at room temperature for typically 15–20 min, the slurry was dissolved in 4.76 g of 0.2 M HCl and stirred until water-clear (about 20 min). Premixing of hexanol and CpCl prior to adding the surfactant is critical to forming the  $L_3$  phase. The weight percent was calculated by summing all reagent weights and then taking the quotient with the weight of 0.2 M HCl. Similar values for solutions made with NaCl(aq) are also given in Table 1.

**Cross-Polarized Optical Studies.** To determine the presence of an ordered anisotropic liquid-crystalline phase, a sample vial was sandwiched between two polarized films that were at 90° angles to each other and placed in front of an intense light. The light source was not completely extinguished by the thin polarizers used, even when fully crossed. Experiments were also performed to test the necessity for vigorous mixing. After HCl(aq) solvent was added, samples were not mixed with a stir bar but were gently mixed by inverting the vial several times before being observed between cross polarizers.

**X-ray Diffraction Characterization.** X-ray diffraction (XRD) characterization of CpCl $\cdot$ H $_2$ O powder was performed using an X-ray diffractometer (Rigaku MSC, Woodlands, TX) with Cu K $\alpha$  X-ray at 40 kV and 30 mA. The scans were done at  $\theta > 3^\circ$  to measure the bilayer spacing and higher-order reflections.

**Small-Angle X-ray Scattering Experiments.** SAXS was used to determine the phase of the solutions prepared by the procedure outlined above. The SAXS experiments were performed at the Cornell High Energy Synchrotron source (CHESS) on the D1 line. In the bending magnetic beamline (D1), W/B $_4$ C multilayer monochromators

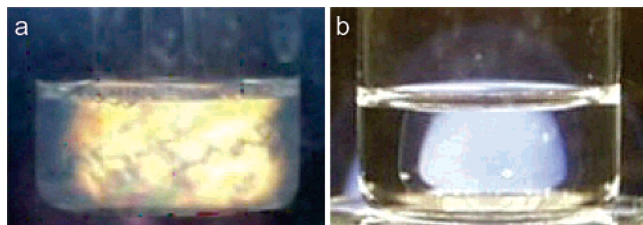


**Figure 3.** Photographs of (a) the birefringence pattern observed for a poorly mixed sample containing an ordered phase and (b) the featureless appearance of a phase-pure  $L_3$  solution. Both images were made on samples held between crossed polarizers. Birefringence indicates the presence of a scattering (e.g., ordered) liquid-crystalline phase. Solutions composed of single-phase  $L_3$  liquid crystal remain optically isotropic and so do not exhibit birefringence. The polarizing films were not thick enough to completely extinguish the intense light source when crossed (more apparent in 3b).

with a bandwidth  $\Delta E/E \approx 1\%$  which gave a photon flux of  $\sim 5 \times 10^{11}$  photons/s $\cdot$ mm $^2$  were used. Thin-walled capillary tubes (Charles Supper Company, Natick, MA) sealed at one end were filled with optically clear solutions of varying solvent concentrations, and the open ends were sealed with wax to prevent solution evaporation. Two-dimensional X-ray images were collected with a  $1024 \times 1024$  pixel CCD (MedOptics Corporation, Tuscon, AZ) with a fiber optic taper (to transfer photons from the phosphor to the CCD chip) and a 5-s read-out time at full resolution.

Digital diffraction images were azimuthally integrated to generate plots of scattered intensity versus  $q = 4\pi \sin \theta / 1.54 \text{ \AA}$  where  $2\theta$  is the angle between the incident and scattered beam directions used to obtain one-dimensional diffraction patterns.

### Results and Discussion

Images of the solutions prepared in the lamellar region, as well as the  $L_3$  region of the CpCl $\cdot$ H $_2$ O/hexanol/HCl(aq) system, are shown in Figure 3. In the lamellar region, solutions appear birefringent under cross-polarizers, whereas for hexanol-to-surfactant ratios larger than that of the  $L_3$  phase, the solution phase separates, indicating a multiphase solution. Premixing of CpCl and hexanol prior to the addition of the solvent is critical to the formation of the  $L_3$  phase. Improper mixing results in the solution being trapped in the lamellar phase, resulting in a colorful birefringence pattern (Figure 3a) which is indicative of an ordered phase within the solution, in contrast to the optically clear solution observed for the  $L_3$  phase (Figure 3b).<sup>1,11</sup> This is attributed to the fact that CpCl $\cdot$ H $_2$ O received as a dry powder has a lamellar structure, verified by XRD (Figure 4). Premixing of CpCl and hexanol allows the partitioning of hexanol into the bilayer which alleviates the strain resulting from the electrostatic repulsion between the ionic surfactant headgroups. The  $L_3$  phase results when hexanol intercalates into the lower-curvature regions of the bilayer, stabilizing the negative curvature of the bilayer ( $c_0 < 0$ ).<sup>22</sup> The negative curvature of the bilayer that results from hexanol permeating into the bilayer makes the Gaussian curvature modulus of the bilayer positive ( $\bar{K} > 0$ ), and the  $L_3$  phase becomes energetically favorable.<sup>1,18</sup>

We compile our results on the isotropic phase region for the two systems investigated, HCl(aq)/CpCl $\cdot$ H $_2$ O/hexanol and NaCl(aq)/CpCl $\cdot$ H $_2$ O/hexanol, in Figure 5. The phase regions for the two systems (Figure 5a) appear generally identical within the range 65–95 wt% solvent content except that the co-surfactant ratio lies between a 1.10 and 1.18 h/c ratio for the HCl(aq) solvent, slightly lower than the same region observed for the system containing 0.2 M NaCl. Within the solvent range from 65 to 55

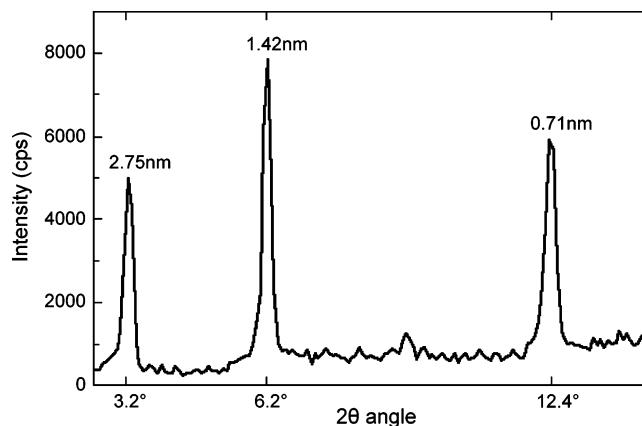


**Figure 4.** X-ray powder diffraction pattern for cetylpyridinium chloride monohydrate. The X-ray pattern at low angles clearly shows that the solid powder has a lamellar structure because the three X-ray peaks shown occur at regular  $d$ -spacings. The second diffraction peak occurs at a  $d$ -spacing that is half of the first peak, and the third peak occurs at a  $d$ -spacing that is one-half of the second one.

wt%, there is a sharp upward shift in the phase field to higher h/c ratios in the HCl(aq) system. Gomati et al. have previously extended the phase diagram of the NaCl(aq) to plot the  $L_3$  phase domain for solvent fractions as low as 46 wt%.<sup>14</sup> They indicate that for solvent concentration between 55 and 85 wt% the  $L_3$  phase domain exists for h/c ratios of  $1.10 \pm 0.2$ , whereas for solvent fractions below 55 wt%, the  $L_3$  phase domain shifts to higher h/c ratios ( $> 1.22$ ).<sup>14</sup> These results indicate that the  $L_3$  phase domain for the 0.2 M NaCl(aq) also shifts upward toward higher h/c ratios in the low-concentration region of the phase diagram. For the HCl(aq) system, this upward shift is observed at solvent fractions  $< 60$  wt% (Figure 5) compared to the 55 wt% for the NaCl(aq) system studied by Gomati et al.<sup>14</sup> This explains why samples prepared with HCl(aq) solvent at concentrations around 60 wt% for h/c ratios of 1.15 would show characteristics of a lamellar structure. Similarly, the phase diagram for the NaCl(aq) system mapped in this work compared with that of the HCl(aq) system, for solvent concentrations higher than 65 wt%, shows a similar upward curve. However, the  $L_3$  phase domain of the two solvent systems remains essentially the same, which leads us to conclude that the substitution of HCl for NaCl does not make a significant difference in the phase diagram (Figure 5b), consistent with our previous assumption.<sup>12,13</sup>

SAXS data on solutions of varying solvent fractions of the HCl(aq)/CpCl $\cdot$ H $_2$ O/hexanol system are shown in Figure 6. The broad scattering patterns of the samples indicate a similar local structure for the different dilutions.<sup>1,4,5,23</sup> Furthermore, the scattering peak shifted with an increased solvent concentration, giving convincing evidence that the  $L_3$  phase exists within these solutions. The 60 wt% solvent exhibits a scattering peak at a reciprocal distance of  $q = 0.11 \text{ \AA}^{-1}$  and hence a characteristic distance of 62.8  $\text{\AA}$ . Similarly, the 70 and 80 wt%  $L_3$  solvent have characteristic spacings of 88.4 and 155  $\text{\AA}$ , respectively. Hence, increasing the amount of solvent relative to the surfactant/co-surfactant content results in an increase in the characteristic spacing, indicating that the solutions follow the universal dilution law.<sup>11</sup> The recorded distances are similar to the ones reported by Gomati et al.<sup>14</sup>

The inset chart in Figure 6 shows the double-logarithmic representation of the one-dimensional scattering patterns. The characteristics of the scattering behavior reveal information of

(22) Gelbart, W. M.; McMullen, W. E.; Masters, A.; Ben-Shaul, A. *Langmuir* **1985**, *1*, 101–103.

(23) Le, T. D.; Olsson, H.; Wennerstrom, H.; Uhrmeister, P.; Rathke, B.; Srey, R. *J. Phys. Chem. B* **2002**, *106*, 9410–9417.



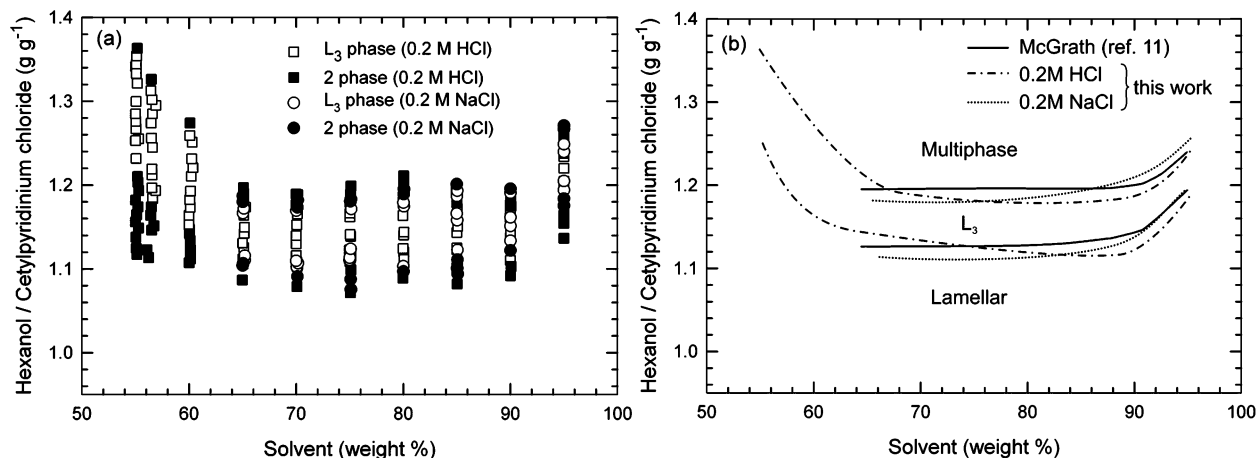


**Figure 5.** (a) Cetylpyridinium chloride monohydrate, hexanol, and 0.2 M HCl phase diagram (squares), and the cetylpyridinium chloride monohydrate, hexanol, and 0.2 M NaCl (circles), in the region of the  $L_3$  phase. This phase diagram extends the region of  $L_3$  phase formation to lower solvent contents than was previously determined. Note the upturn in the  $L_3$  phase region (to higher hexanol/cetylpyridinium chloride monohydrate ratios) at the extremes of the solvent weight percent. The regions marked as two-phase (filled squares and circles) showed either lamellar phases, as observed through crossed polarizers (Figure 3), were observed by the naked eye to be cloudy or to form distinct layers. (b) Superimposing the  $L_3$  phase fields from this study (dashed lines) on the  $L_3$  phase as described by McGrath (solid black lines) reveals very little difference in the shape or extent of the  $L_3$  region regardless of the source of the chloride ion. Our results using NaCl(aq) solvent corroborates the original study done by McGrath using brine solutions (ref 11).

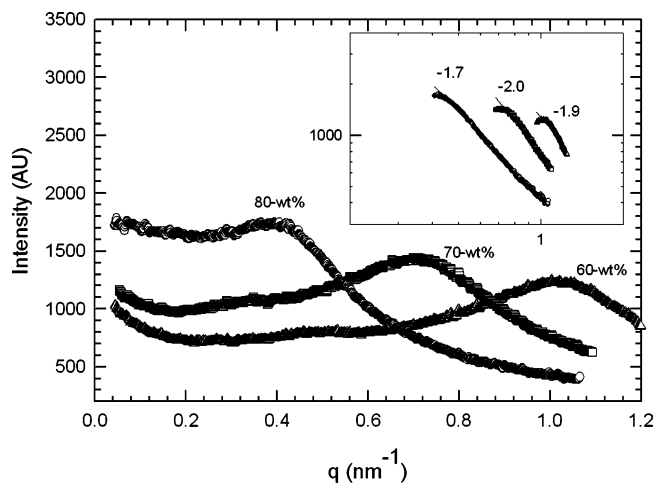


**Figure 6.** Small-angle X-ray scattering pattern for the solutions of hexanol/CpCl·H<sub>2</sub>O and 0.2 M HCl solvent (pH ≈ 0.7). Solutions with increasing solvent concentrations follow the swelling behavior, as indicated by the shift in the scattering peak. A log–log plot of the scattering profiles is used to check the  $q^{-2}$  decaying behavior (inset). The slopes of the lines are  $-1.7$  for 80 wt% solvent,  $-2.0$  for 70 wt% solvent, and  $-1.9$  for 60 wt% solvent.

the structure of the solution at various length scales. At the small  $q$  values, the scattering intensity (not shown here) is constant since the inhomogeneities within the sample cannot be probed at the corresponding larger length scales. At intermediate distances, the intensity has a limiting behavior of  $q^{-2.4}$ ,  $q^{-2.1}$ , and  $q^{-1.8}$  for the 60, 70, and 80 wt%  $L_3$  solutions, respectively. The limiting behavior of the intensity as a function of the reciprocal distance,  $q$ , can be used to determine the spatial arrangement of the networks.<sup>24</sup> The power law exponent is related to the fractal dimension if the cluster size dimension obeys a power law and the aggregates are self-similar as in the case of the  $L_3$  phase.<sup>24,25</sup> Bilayer structures such as the  $L_\alpha$  and the  $L_3$  phases are known to follow a  $q^{-2}$  dependence. Here,  $L_3$  phases of the three solvent fractions exhibit a limiting behavior dependence of  $\sim q^{-2}$ , indicating a local bilayer structure within the solutions. Both the broad scattering pattern and the limiting behavior of the intensity

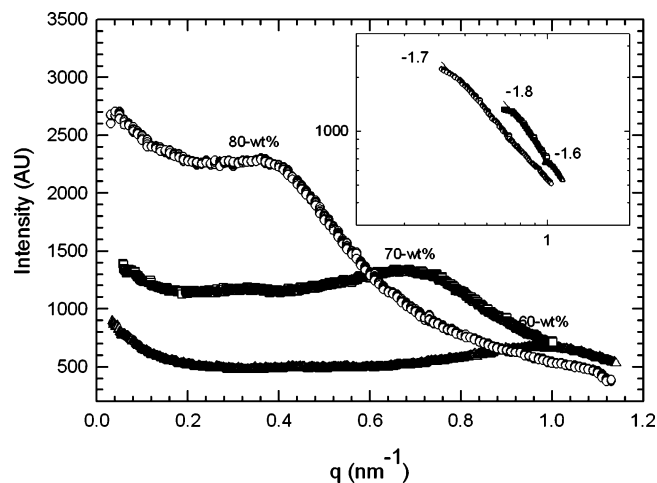


**Figure 7.** Small-angle X-ray scattering pattern for the solutions of hexanol/CpCl·H<sub>2</sub>O and 0.2 M HCl and 0.2 M NaCl solvent (pH 2). Solutions with increasing solvent concentrations follow the swelling behavior, as indicated by the shift in the scattering peak. A log–log plot of the scattering profiles is used to check the  $q^{-2}$  decaying behavior (inset). The slopes of the lines are  $-1.7$  for 80 wt% solvent,  $-1.8$  for 70 wt% solvent, and  $-1.6$  for 60 wt% solvent.

confirm the formation of the  $L_3$  phase. Figure 7 shows the scattering pattern of three concentrations of the  $L_3$  mesophase synthesized at pH 2. The data confirm that replacing the pH ≈ 1 solvent with a pH 2 solvent of identical ionic strength does not disrupt the phase formation. The shift in the peak position with an increase in solvent concentration indicates the presence of the dilution law characteristic of a structure in this phase region. Furthermore, the inset shows the same  $q^{-2}$  limiting behavior as seen of the solution prepared at pH 0.7.

Although the similarity of the two different phase diagrams may seem coincidental, this can be explained by noting that the specific structure of the  $L_3$  or sponge phase is a result of the density of curvature free energy of the surfactant bilayer. As mentioned previously, a significant contribution to this free energy is made by electrostatic interactions between the pyridinium ion headgroups in CpCl·H<sub>2</sub>O.<sup>17</sup> Changes in the electrostatic interactions between headgroups do alter the curvature free energy density and can result in different surfactant mesophases being

(24) Schaefer, D. W. *Science* **1989**, *243*, 1023–1027.

more thermodynamically favored. Therefore, the fact that a similar phase diagram for the formation of  $L_3$  from  $\text{CpCl}\cdot\text{H}_2\text{O}$ /hexanol is observed when either 0.2 M HCl or 0.2 M NaCl is used as solvent implies that, in either solvent, the electrostatic interactions between headgroups are similar.

To understand why the electrostatic interactions are similar, we consider that changes in the composition of ions in the solvent can alter such interactions in two ways. First, changes in pH can alter the degree of ionization of the headgroups. The pH of the HCl solution will be strongly acidic, relative to that of the NaCl solution. However, the degree of ionization of the headgroup of  $\text{CpCl}\cdot\text{H}_2\text{O}$  is independent of pH. A decrease in pH will have no effect on the degree of ionization of the pyridinium ions and thus the electrostatic interactions between headgroups. Second, changes in the ionic strength of the solvent can alter the interaction free energy between headgroups. This second effect can be described accurately using the Poisson–Boltzmann equation.<sup>26</sup> Since only the concentration and valence (charge number) of ions appear in this mean field theoretical model, the specific chemical identity of the ions is irrelevant.<sup>26</sup> HCl(aq) is a strong acid and will completely dissociate in water to form  $\text{H}_3\text{O}^+$  and  $\text{Cl}^-$  ions, whereas NaCl completely dissociates to form  $\text{Na}^+$  and  $\text{Cl}^-$ . Therefore, the ionic strength of the two solutions will be identical; from the Poisson–Boltzmann theory, we can predict that the electrostatic interactions between headgroups will be

(25) Martin, J. E. *J. Appl. Crystallogr.* **1986**, *19*, 25–27.

(26) Daicic, J.; Fogden, A.; Carlsson, I.; Wennerstrom, H.; Jonsson, B. *Phys. Rev. E* **1996**, *54*, 3984–3998.

unchanged in going from a solvent composed of 0.2 M NaCl to one composed of 0.2 M HCl. Similarly, for the pH 2 solvent, the ionic strength of the solvent is maintained at 0.2 M  $\text{Cl}^-$  ions; therefore, the electrostatic interactions between the surfactant headgroups remain unchanged, and the phase behavior and characteristic distances of the structure remains the same.

### Conclusions

We have mapped the respective phase diagrams for two solution systems, one using brine solvent and the other using 0.2 M hydrochloric acid in the region of the  $L_3$  phase. Using cross-polarized optics and SAXS, we conclude that decreasing the solvent pH by  $\sim 6$  pH units does not make a significant difference in the phase diagram. This is attributed to the equivalent ionic strength of the three pH solvents and to the fact that both HCl(aq) and NaCl(aq) dissociate completely in water, producing a similar effect on the degree of ionization of the pyridinium ions and thus the electrostatic interactions between headgroups.

**Acknowledgment.** The work was partially supported by NASA Grant No. NAG-2-1475 and by the NASA University Research, Engineering, and Technology Institute on BioInspired Materials (BIMat) under Award No. NCC-1-02037. Additional support was provided by the National Science Foundation under Grants No. CTS-0003882 and CTS-0134429. We wish to thank Arthur Woll of CHESS, Cornell University for assistance in running the SAXS and in the interpretation of the data.

LA0522449